# Synthesizing Sparse and Delay-Robust Distributed Secondary Frequency Controllers for Microgrids

Sultan Alghamdi, Johannes Schiffer and Emilia Fridman

***Abstract*—Consensus-based control schemes experience increasing popularity in the context of secondary frequency control in microgrids. Fundamental aspects in their practical implementation are the design of the communication topology as well as robustness with respect to both time-varying communication delays and exogenous disturbances. Motivated by this, we propose a design procedure for a consensus-based secondary frequency controller that ensures robustness with respect to heterogeneous fast-varying communication delays and simultaneously provides the option to trade off the $L_2$-gain performance against the number of required communication links. Our design criterion is equilibrium-independent and based on the Lyapunov-Krasovskii method for interval time-varying delays together with the descriptor method. The efficacy of the proposed approach is demonstrated via numerical experiments on the CIGRE benchmark medium voltage distribution network.**

***Index Terms*—Microgrids, microgrid stability, smart grid applications, secondary control, consensus algorithms, multi-agent systems, distributed cooperative control, time-delay systems.**

## I. Introduction

### A. Motivation and Related Work

THE increasing penetration of economic and environmentally friendly renewable energy resources (RESs) introduces enormous challenges for conventional power systems operation and control [1]. Most RESs are small-scaled distributed generation (DG) units, which are connected to the medium (MV) and low voltage (LV) levels via power electronics converters. Therefore, the replacement of a few bulk conventional fossil fuel based power plants with a large number of small-scale DGs significantly increases the complexity of balancing demand and generation in real-time. Clearly, in such a setting, centralized operating schemes are inappropriate and instead distributed architectures need to be developed.

One of the most promising approaches to ease the integration of DGs in the electrical grid is the microgrid (MG) concept [1], [2]. A MG is a small-scale power system, which is composed of a combination of DG units, energy storage devices and loads at the distribution level. MGs can be either connected to the main grid through a point of common coupling (PCC) or operated autonomously, i.e., in islanded mode [1], [3]. Thus, future power systems could be operated as a cell-structure of interconnected MGs [4].

In AC MGs, most of the RESs are DC sources and therefore DC/AC inverters are usually required to interface the generation units to an AC network. In such scenarios it is important to recognize that the inverters' physical dynamics significantly differ from conventional synchronous generator dynamics [5] and the increasing integration of inverter-interfaced units results in a reduced system inertia. The latter facts imply that new concepts and strategies to control MGs and ensure their reliable and stable operation are needed. Thus, for this type of networks many new control challenges arise. Among these, frequency regulation is a very fundamental operational objective [2], [6] to which the present paper is dedicated.

As in bulk power systems [7], in MGs frequency regulation is typically realized via a hierarchical control layer consisting of primary, secondary and tertiary control [8]. The primary controllers are usually implemented in a completely decentralized manner to ensure frequency stability and power sharing. However, a well-known drawback of primary control is a steady state frequency deviation from its nominal value [8]. Thus, secondary frequency control action is required for frequency restoration. Finally, tertiary control is mainly concerned with energy management.

In conventional power systems, secondary frequency control is implemented via a centralized automatic generation control (AGC) [7]. However, due to the dispersed nature of generation units and the required operational flexibility, in MGs usually distributed algorithms are preferred for secondary control tasks. In particular, distributed consensus-based algorithms have gained increasing popularity for secondary frequency control in MGs in recent years [9]–[13]. Consensus protocols are distributed protocols, and peer-to-peer communication between participating units is essential for their implementation [14]. Consequently, the properties of the employed communication network, such as its topology or transmission delays, may severely affect the overall closed-loop MG dynamics and can even lead to instability [2]. In addition to communication uncertainties, the electrical dynamics of the MG is also continuously exposed to perturbations, e.g., in the power demand. Therefore, these three aspects (shape of the communication topology, delay robustness and disturbance attenuation) should be taken into account already at the design stage of any distributed frequency controller.

Delay-robustness of consensus-based secondary controllers has been investigated in [15]–[19], but the analysis is ei-

S. Alghamdi is with School of Electronic & Electrical Engineering, University of Leeds, United Kingdom, LS2 9JT elsalg@leeds.ac.uk

J. Schiffer is with Control Systems and Network Control Technology, Brandenburg University of Technology (BTU), 03046, Cottbus, Germany schiffer@b-tu.de.

E. Fridman is with Tel-Aviv University, Israel emilia@tauex.tau.ac.il

J. Schiffer acknowledges funding from the European Union's Horizon 2020 research and innovation programme under the Marie Skłodowska-Curie grant agreement No. 734832 and E. Fridman acknowledges funding from the Israel Science Foundation (grant no. 673/19).

ther limited to a linearized (small-signal) model or does not consider the electrical dynamics and is partially restricted to constant delays. In [20], stability conditions for a distributed averaging secondary frequency controller have been derived under consideration of fast-varying time-delays and a dynamic communication topology, but the (nominal) communication topology is assumed to be fixed a priori and no external perturbations are considered.

Bounded input-output performance of linearized models of secondary controlled MGs has been considered using the $H_2$-norm in [13] and the $H_1$-norm in [21], [22]. A very similar setup for bulk power systems with distributed frequency control is employed in [12], where in addition to minimizing the $H_2$-norm also sparsity of the communication network is promoted. The interaction between the cyber and physical layers of a related primal-dual distributed secondary control scheme has recently been explored in [23] by using a linearized power system model with uniform inertia and damping coefficients.

In summary, the aspects of delay robustness, disturbance attenuation and communication topology design have to some extent been considered in the literature, but mainly on an individual basis and by using linearized MG models. In particular, there are no available approaches, which jointly address all three aspects. Yet, clearly, from a practical point of view the development of holistic design criteria, which takes into account the physical and cyber layers of the system, is highly desirable to further facilitate a robust and efficient implementation of consensus-based secondary controllers in MGs. This motivates the work in the present paper.

### B. Contributions

As a consequence of the above discussion, the main contribution in this paper is a synthesis for distributed secondary frequency controllers in MGs in form of a convex optimization problem with linear matrix inequality (LMI) constraints. The derived design criterion guarantees robustness with respect to time-varying heterogeneous communication delays, while providing the option to shape the closed-loop performance by trading off the $L_2$-gain performance and the number of communication links.

The controller synthesis is developed for a nonlinear MG model and, as common in sampled-data networked control systems [24]–[26], accounts for heterogeneous time-varying communication delays. Thereby, we model the delays as interval time-varying delays, i.e., assuming non-zero constant upper and lower bounds [26]. This is in contrast to our previous related work [20], [27], where a lower delay bound of zero is assumed, and represents a more accurate delay model, since any signal transmitted over a communication network experiences a minimum delay. In addition, we also show via numerical examples that modeling the delays as interval time-varying delays can lead to less conservative results compared to those reported in [27]. With regard to external disturbances, the proposed design procedure ensures disturbance attenuation by minimizing the upper bound of the $L_2$-gain, which we recall is defined as the maximum energy amplification ratio of the system and the counterpart to the $H_1$-norm for nonlinear systems [26], [28].

In addition to disturbance and delay robustness another highly relevant aspect in the control design is considered in our synthesis, namely the choice of the communication topology. Besides [12], in all other work on consensus-based frequency control, see [13], [15]–[22], merely a connected communication graph is assumed, but no further recommendations on how the actual communication topology should be chosen are made. However, this is a crucial facet in any practical implementation. Of particular interest is to quantify the benefits arising from increasing the number of communication links beyond a merely connected topology. Therefore, inspired by related work on sparsity-promoting control for bulk power systems [12], [29]–[31], we integrate this aspect in our synthesis by employing the (re)weighted $\ell_1$-norm as a proxy for the sparsity of the communication network [32]. The achievable benefit is quantified in terms of the $L_2$-gain performance of the closed-loop system.

Our design criterion is derived based on the Lyapunov-Krasovskii (LK) and the descriptor methods [25], [26]. We remark that, compared to the related work [20], combining the descriptor method with the LK method is essential to be able to obtain a controller synthesis in terms of LMIs, which can be evaluated with efficient numerical methods [33]. Furthermore, compared to a design based on linearization, our criterion does not require prior knowledge of the operating point (besides the usual requirement that the stationary angle differences do not exceed $\frac{\pi}{2}$). Thus, the performance properties provided by our design hold true in a wide range of operating conditions.

Another important contribution in the paper is to illustrate the proposed synthesis via a two-step design study on the CIGRE benchmark medium voltage (MV) distribution network [34]. In particular, we demonstrate how the weighting coefficients in the cost function can be used to shape the sparsity of the controller as well as the robustness and convergence speed of the resulting closed-loop system.

The main advances of the present paper compared to our previous work [27] are as follows. We consider heterogeneous fast-varying communication delays rather than a uniform delay and model them as interval ones. As shown in the numerical examples, this allows to reduce the conservativeness of our stability conditions, but also requires the development of a new Lyapunov-Krasovskii functional (LKF). Furthermore, we provide extensive numerical experiments, including an investigation on the relationship between the sparsity pattern of the network Laplacian matrix and the main weighting matrix in the secondary frequency controller.

The remainder of this paper is structured as follows. In Section II, we recall some preliminaries on the $L_2$-gain of dissipative systems and graph theory. The MG model and the consensus-based secondary control law are introduced in Section III. In Section IV, we propose a controller synthesis ensuring robustness with respect to heterogeneous fast-varying delays as well as disturbance rejection, while minimizing the number of communication links. A numerical example to demonstrate the effectiveness of the approach is given in Section V. A brief summary and topics of future work are

provided in Section VI.

**Notation.** We define the sets $\mathbb{R}_{\geq 0} := \{x \in \mathbb{R} | x \geq 0\}$, $\mathbb{R}_{>0} := \{x \in \mathbb{R} | x > 0\}$ and $\mathbb{R}_{<0} := \{x \in \mathbb{R} | x < 0\}$. For a set $\mathcal{V}$, $|\mathcal{V}|$ denotes its cardinality and $[\mathcal{V}]^k$ denotes the set of all subsets of $\mathcal{V}$ that contain $k$ elements. Let $x := \mathrm{col}(x_i) \in \mathbb{R}^n$ denote a vector with entries $x_i$ for $i = 1, \ldots, n$, $\mathbb{1}_n$ the vector with all entries equal to one, $I_n$ the $n \times n$ identity matrix, $0$ a zero matrix of appropriate dimensions and $\mathrm{diag}(a_i); i = 1, \ldots, n$, an $n \times n$ diagonal matrix with diagonal entries $a_i \in \mathbb{R}$. For $A \in \mathbb{R}^{n \times n}$, $A > 0$ ($A < 0$) means that $A$ is symmetric positive (negative) definite. The lower-diagonal elements of a symmetric matrix are denoted by $*$. The Euclidean norm of a vector $x \in \mathbb{R}^n$ is denoted by $\|x\|_2$. We denote by $W[-h, 0]$, $h \in \mathbb{R}_{>0}$, the Banach space of absolutely continuous functions $\phi : [-h, 0] \to \mathbb{R}^n$, with $\dot{\phi} \in L_2(-h, 0)^n$ and with the norm $\|\phi\|_W = \max_{\theta \in [-h,0]} |\phi(\theta)| + \left(\int_{-h}^{0} |\dot{\phi}(\theta)|^2 d\theta\right)^{0.5}$. Also, $\nabla f$ denotes the gradient of a function $f : \mathbb{R}^n \to \mathbb{R}$.

## II. Preliminaries

### A. $L_2$-Gain of Dissipative Systems

We briefly recall some standard results on dissipative systems based on [28], [35]. Consider the state space system

$$\Sigma : \begin{cases} \dot{x} = f(x, u), \\ y = h(x, u) \end{cases}; \tag{II.1}$$

with $x \in \mathbb{R}^n$, $u \in \mathbb{R}^m$ and $y \in \mathbb{R}^p$.

A signal $u : \mathbb{R}_{\geq 0} \to \mathbb{R}^m$ is in $L_2$ if its $L_2$-norm $\|u\|_{L_2}$, given by

$$\|u\|_{L_2} = \sqrt{\int_0^\infty u^\top(t) u(t) dt},$$

is finite. The extended $L_2$-space $L_{2e}$ is defined by

$$L_{2e} = \{u \mid u_\tau \in L_2 \ \forall \tau \in [0, \infty)\},$$

where $u_\tau$, $\tau \in [0, \infty)$, is the truncation of $u$ defined by

$$u_\tau = \begin{cases} u(t), & 0 \leq t \leq \tau \\ 0, & t > \tau \end{cases}.$$

We employ the following notions.

**Definition II.1.** *The state space system $\Sigma$ is said to have finite $L_2$-gain if there exist finite nonnegative constants $\gamma$ and $b$, such that for all $x_0 = 0$ and for all $u \in L_{2e}$,*

$$\|y\|_{L_2} \leq \gamma \|u\|_{L_2} + b.$$

**Definition II.2.** *The state space system $\Sigma$ is dissipative with respect to the supply rate $s : \mathbb{R}^m \times \mathbb{R}^q \to \mathbb{R}$ if there exists a function $S : \mathbb{R}^n \to \mathbb{R}_{\geq 0}$, called the storage function, such that for all $t_1 \geq t_0$ and all input functions $u$,*

$$S(x(t_1)) \leq S(x(t_0)) + \int_{t_0}^{t_1} s(u(t), y(t)) dt.$$

**Definition II.3.** *The state space system $\Sigma$ has a $L_2$-gain less than or equal to $\gamma$ if it is dissipative with respect to the supply rate $s(u, y) = \frac{1}{2}(\gamma^2 \|u\|_2^2 - \|y\|_2^2)$. The $L_2$-gain of $\Sigma$ is defined as $\gamma(\Sigma) = \inf\{\gamma \mid \Sigma \text{ has } L_2\text{-gain } \gamma\}$.*

Based on [28, Definition 6.2], we employ the following notion of a *small-signal* $L_2$-gain.

**Definition II.4.** *The state space system $\Sigma$ has a small-signal $L_2$-gain less than or equal to $\gamma$ if it is dissipative with respect to the supply rate $s(u, y) = \frac{1}{2}(\gamma^2 \|u\|_2^2 - \|y\|_2^2)$ for all $u \in L_2^m$ with $\sup_{0 \leq t < \infty} \|u\|_2 \leq r$ for some positive real constant $r$.*

### B. Algebraic Graph Theory

An undirected weighted graph of order $n$ is a triple $\mathcal{G} = (\mathcal{V}, \mathcal{E}, z)$, with set of nodes $\mathcal{V} = \{1, \ldots, n\}$, set of undirected edges $\mathcal{E} \subseteq [\mathcal{V}]^2$, $\mathcal{E} = \{e_1, \ldots, e_m\}$, $m = |\mathcal{E}|$ and weight function $z : \mathcal{E} \to \mathbb{R}_{\geq 0}$. By associating an arbitrary ordering to the edges, the node-edge incidence matrix $B \in \mathbb{R}^{|\mathcal{V}| \times |\mathcal{E}|}$ of an undirected graph is defined element-wise as $b_{il} = 1$, if node $i$ is the source of the $l$-th edge $e_l$, $b_{il} = -1$, if $i$ is the sink of $e_l$ and $b_{il} = 0$ otherwise. The Laplacian matrix of an undirected weighted graph is given by [36], [37]

$$L = BZB^\top, \quad Z = \mathrm{diag}(z_l), \tag{II.2}$$

where $z_l \neq 0$ is the weight of the $l$-th edge, $l = 1, \ldots, m$. An ordered sequence of nodes such that any pair of consecutive nodes in the sequence is connected by an edge is called a path. A graph $\mathcal{G}$ is called connected if for all pairs $\{i, k\} \in [\mathcal{V}]^2$ there exists a path from $i$ to $k$. The Laplacian matrix $L$ of an undirected graph is positive semidefinite with a simple zero eigenvalue if and only if the graph is connected. The corresponding right eigenvector to this simple zero eigenvalue is $\mathbb{1}_n$, i.e., $L\mathbb{1}_n = 0_n$ [37]. We refer the reader to [36], [37] for further information on graph theory.

## III. Microgrid Model with Distributed Secondary Frequency Control and Heterogeneous Time Delays

### A. Microgrid Model

We consider a MG with mixed generation pool consisting of rotational and electronic interfaced units. Following standard practice we assume that a Kron-reduction has been carried out [7] and denote the set of network nodes by $\mathcal{N} = \{1, \ldots, n\}$, $n \geq 1$. Furthermore, we assign a phase angle $\theta_i : \mathbb{R}_{\geq 0} \to \mathbb{R}$ and a frequency $\omega_i = \dot{\theta}_i$ to each unit in the MG, $i \in \mathcal{N}$. In addition, as usual when considering secondary frequency control [9], [20], we assume constant voltage amplitudes $V_i \in \mathbb{R}_{>0}$, $i \in \mathcal{N}$, and a lossless network. The latter assumption is acceptable whenever the inverter output (and transformer) impedance is highly inductive, which in particular applies to MV MGs [38]. With these assumptions, two nodes $i$ and $k$ are connected via a non-zero susceptance $B_{ik} \in \mathbb{R}_{<0}$. If there is no line between $i$ and $k$, then $B_{ik} = 0$. We denote the set of neighboring nodes of node $i$ by $\mathcal{N}_i = \{k \in \mathcal{N} \mid B_{ik} \neq 0\}$. Furthermore, we assume a connected electrical network i.e., we assume that for all $\{i, k\} \in [\mathcal{N}]^2$ there exists an ordered sequence of nodes from $i$ to $k$ such that any pair of consecutive nodes in the sequence is connected by a power line represented by an admittance.

It is convenient to define the vectors $\theta = \mathrm{col}(\theta_i)$ and $\omega = \mathrm{col}(\omega_i)$ as well as the potential function $U : \mathbb{R}^n \to \mathbb{R}$,

$$U(\theta) = \sum_{\{i,k\} \in [N]^2} |B_{ik}| V_i V_k \cos(\theta_{ik}).$$

Then the active power flows $P : \mathbb{R}^n \to \mathbb{R}^n$ can be compactly written as

$$P(\theta) = \nabla U(\theta).$$

With regard to primary control, we assume that all units are equipped with the standard frequency droop controller [6], [7], [39]. Then, the MG dynamics are given by [38], [39]

$$\begin{aligned} \dot{\theta} &= \omega, \\ M\dot{\omega} &= -D(\omega - 1_n \omega^d) - \nabla U(\theta) + P^{\mathrm{net}} + u, \end{aligned} \tag{III.1}$$

where $D = \mathrm{diag}(D_i) \in \mathbb{R}^n_{>0}$ is the matrix of (inverse) droop coefficients, $\omega^d \in \mathbb{R}_{>0}$ is the reference frequency and $u : \mathbb{R}_{\geq 0} \to \mathbb{R}^n$ is the secondary frequency control input. Moreover, the matrix of (virtual) inertia coefficients is given by $M = \mathrm{diag}(M_i) \in \mathbb{R}^n_{>0}$, where for any inverter-interfaced unit $M_i = \tau_i D_i$ with $\tau_i \in \mathbb{R}_{>0}$ being the time constant of the power measurement filter. In addition, $P^{\mathrm{net}}$ is given by $P^{\mathrm{net}} = \mathrm{col}(P_i^d - G_{ii} V_i^2)$, where $P_i^d \in \mathbb{R}$ denotes the active power set point and $G_{ii} V_i^2$; $G_{ii} \in \mathbb{R}_{\geq 0}$, represents the active power demand at the $i$-th node. See [3] for further details on the modeling of the system components.

### *B. Secondary Frequency Control: Objectives and Distributed Control Scheme*

Suppose that the solutions of the system (III.1) evolve along a motion with constant frequency $\omega^s = 1_n \omega^*$; $\omega^* \in \mathbb{R}$. Then,

$$1_n^\top M \dot{\omega}^s = 0 \quad \Rightarrow \quad \omega^* = \omega^d + \frac{1_n^\top P^{\mathrm{net}} + 1_n^\top u}{1_n^\top D 1_n}; \tag{III.2}$$

where we have used the fact that $1_n^\top \nabla U(\theta) = 0$. A standard requirement in power system operation is that $\omega^* = \omega^d$; i.e., the network synchronizes to the nominal frequency [6], [7]. However, in practice, the load demands $G_{ii} V_i^2$ contained in $P^{\mathrm{net}}$ are unknown and thus, typically, $1_n^\top P^{\mathrm{net}} \neq 0$. Therefore, the control inputs $u$ have the task to compensate this power imbalance such that indeed $\omega^* = \omega^d$; see (III.2). This task is termed secondary frequency control [6], [7].

Let $A \in \mathbb{R}^n_{>0}{}^n$ be a diagonal positive definite weighting matrix, $K \in \mathbb{R}^n_{>0}{}^n$ be a diagonal feedback gain matrix and $L \in \mathbb{R}^n{}^n$ be the Laplacian matrix of an undirected and connected graph with incidence matrix $B$ and diagonal matrix of nonnegative edge weights $Z$, see (II.2). Consider the distributed secondary frequency control [9], [20], [40]

$$\begin{aligned} u &= -p, \\ \dot{p} &= K(\omega - 1_n \omega^d) + KALAp. \end{aligned} \tag{III.3}$$

Due to its distributed nature, the secondary control law (III.3) is prone to be affected by communication delays [2], [24]. Moreover, in a practical communication-based control there will always be a certain minimum communication delay between different agents, i.e., in our case generation units [41]. As a consequence of this fact, we model the delay, which affects the information sent from node $i$ to node $k$ over the edge $\{i,k\}$, by an interval (or non-small) delay [26]

$$\tau_{ik} : \mathbb{R}_{\geq 0} \to [h_{0_{ik}}, h_{1_{ik}}],$$

with upper and lower bounds $0 < h_{0_{ik}} \leq h_{1_{ik}}$. In addition, our subsequent analysis also accounts for asymmetric delays, i.e., $\tau_{ik} \neq \tau_{ki}$. Furthermore, as is shown via numerical examples in Section V, modeling the delays as interval time-varying delays also permits to reduce the conservativeness of our conditions compared to those reported in our previous work [27], where we assumed a uniform delay with a lower bound of zero, i.e., $h_{0_{ik}} = 0$. The corresponding control error $e_{ik}$ is then computed as [14], [42]

$$e_{ik}(t) = A_{ii} p_i(t - \tau_{ik}(t)) - A_{kk} p_k(t - \tau_{ik}(t)). \tag{III.4}$$

As standard practice in sampled-data systems [25], [26], the delay $\tau_{ik}$ can be piecewise-continuous in $t$ and fast-varying, i.e no restrictions on the existence, continuity, or boundedness of $\dot{\tau}_{ik}(t)$ are imposed.

In order to obtain a compact representation of the closed-loop system, we introduce the matrices $B_r \in \mathbb{R}^{|V| \times |E|}$, $r = 1, \ldots, 2m$, where $m = |E|$ is the number of edges of the undirected graph. Since we allow for $\tau_{ik}(t) \neq \tau_{ki}(t)$, we require $2m$ matrices $B_r$ to represent all delayed information flows in the network. The matrices $B_r$ are defined as follows. If node $i$ is the source of the $r$-th edge $\{i,k\}$ and the information flow is affected by the delay $\tau_r(t) = \tau_{ik}(t)$, then $b_{ri} = 1$ and all other entries of $B_r$ are zero. If node $i$ is the sink of the $r$-th edge $\{i,k\}$ and the information flow is affected by the delay $\tau_r(t) = \tau_{ik}(t)$, then $b_{ri} = -1$ and all other entries of $B_r$ are zero. Hence,

$$\sum_{r=1}^{2m} B_r Z B^\top = L$$

and by introducing

$$T_r = B_r Z B^\top; \tag{III.5}$$

the control law in (III.3) can be written compactly as

$$\dot{p} = K(\omega - 1_n \omega^d) - KA \sum_{r=1}^{2m} T_r A p(t - \tau_r). \tag{III.6}$$

It has been shown in [40], [43], [44], that in addition to being able to restore the frequency to its nominal value, the control (III.6) also ensures economic optimality in a synchronized state, i.e.,

$$A_{ii} u_i^s = A_{kk} u_k^s \quad \forall i \in N, \quad \forall k \in N.$$

Thus, usually the matrix $A$ is fixed by economic considerations.

Hence, given (III.6), the distributed secondary control design problem consists in suitably determining the matrices $K$ and $Z$. This problem is addressed in the present paper.

### C. Closed-Loop System

Combining (III.1) with (III.6) yields

$$\begin{aligned} \dot{\vartheta} &= \omega; \\ M\dot{\omega} &= -D(\omega - \mathbf{1}_n\omega^d) - rU(\vartheta) + P^{\text{net}} - p; \\ \dot{p} &= K(\omega - \mathbf{1}_n\omega^d) - KA\sum_{r=1}^{2m} T_r A p(t-\tau_r). \end{aligned} \tag{III.7}$$

For the subsequent controller synthesis, the following notion is useful, see also [20], [38].

**Definition III.1.** *The system* (III.7) *admits a synchronized motion if it has a solution for all $t \geq 0$ of the form*

$$\vartheta^s(t) = \vartheta_0^s + \omega^s t, \quad \omega^s = \omega - \mathbf{1}_n\omega^d, \quad p^s \in \mathbb{R}^n,$$

*where $\omega^d \in \mathbb{R}$ and $\vartheta_0^s \in \mathbb{R}^n$ are such that*

$$|\vartheta_{0;i}^s - \vartheta_{0;k}^s| < \frac{\pi}{2} \quad \forall i \in \mathcal{N}, \forall k \in \mathcal{N}_i.$$

We note that the system (III.7) possesses at most one synchronized motion and that this motion satisfies [40], [43], [44]

$$u^s = p^s, \quad p^s = \gamma A^{-1}\mathbf{1}_n, \quad \gamma = \frac{\mathbf{1}_n^\top P^{\text{net}}}{\mathbf{1}_n^\top A^{-1}\mathbf{1}_n}. \tag{III.8}$$

## IV. Controller Synthesis

### A. Coordinate Transformation and Error System

We perform both a coordinate transformation and reduction that are instrumental to our synthesis. Let $K = \kappa K$, where $K \in \mathbb{R}^{n\times n}$ is a diagonal matrix with positive diagonal entries and $\kappa > 0$ is a parameter. Note that the fact that $\sum_{r=1}^{2m} T_r\mathbf{1}_n = L\mathbf{1}_n = 0_n$ leads to an invariant subspace in the $p$-variables, which highly complicates the design of a strict LKF for the dynamics (III.7). Thus, to develop the controller synthesis in the presence of fast-varying delays the following coordinate transformation with $p \in \mathbb{R}^{n-1}$ and $\chi \in \mathbb{R}$ is employed to eliminate this invariant subspace

$$p = W^\top(\kappa K)^{\frac{1}{2}}\vartheta; \quad W = \begin{bmatrix} W & \frac{1}{\sqrt{n}}\kappa^{-\frac{1}{2}}A^{-\frac{1}{2}}\mathbf{1}_n \end{bmatrix}; \tag{IV.1}$$

where $W \in \mathbb{R}^{n\times(n-1)}$ is chosen such that $W^\top K^{\frac{1}{2}}A^{-1}\mathbf{1}_n = 0_{n-1}$, and $\chi = \kappa K^{\frac{1}{2}}A^{-1}\mathbf{1}_n k_2^2$. Hence, the column vectors of $W$ form an orthonormal basis that is orthogonal to $K^{\frac{1}{2}}A^{-1}\mathbf{1}_n$ and, thus, the transformation matrix $W \in \mathbb{R}^{n\times n}$ is orthogonal, i.e.,

$$WW^\top = WW^\top + \frac{1}{n}\kappa^{-1}K^{\frac{1}{2}}A^{-1}\mathbf{1}_n\mathbf{1}_n^\top K^{\frac{1}{2}}A^{-1} = I_n. \tag{IV.2}$$

From (IV.1) we have that

$$\vartheta = \sqrt{n}\,\kappa^{-\frac{1}{2}}\mathbf{1}_n^\top A^{-1}K^{-1}p. \tag{IV.3}$$

By using (III.7) together with the fact $\sum_{r=1}^{2m} T_r\mathbf{1}_n = 0_n$, we obtain

$$\dot{\vartheta} = \sqrt{n}\,\kappa^{-\frac{1}{2}}\mathbf{1}_n^\top A^{-1}(\omega - \mathbf{1}_n\omega^d);$$

which by integrating with respect to time and recalling (IV.3) yields

$$\begin{aligned} \vartheta &= \sqrt{n}\,\kappa^{-\frac{1}{2}}\mathbf{1}_n^\top A^{-1}(\vartheta_0 - \mathbf{1}_n\omega^d t + \gamma K^{-1}p_0) \\ &= \sqrt{n}\,\kappa^{-\frac{1}{2}}\mathbf{1}_n^\top A^{-1}\vartheta - \mathbf{1}_n\omega^d t + \vartheta_0; \end{aligned} \tag{IV.4}$$

where

$$\vartheta_0 = \sqrt{n}\,\kappa^{-\frac{1}{2}}\mathbf{1}_n^\top A^{-1}\vartheta - \gamma K^{-1}p_0 - \vartheta_0. \tag{IV.5}$$

Thus,

$$\begin{aligned} p &= (\kappa K)^{\frac{1}{2}}Wp + \frac{1}{\sqrt{n}}(\kappa K)^{\frac{1}{2}}K^{\frac{1}{2}}A^{-1}\mathbf{1}_n\chi; \\ &= (\kappa K)^{\frac{1}{2}}Wp + -A^{-1}\mathbf{1}_n\mathbf{1}_n^\top A^{-1}(\omega - \mathbf{1}_n\omega^d t) \\ &\quad + \sqrt{n}\,\kappa^{-\frac{1}{2}}A^{-1}\mathbf{1}_n\vartheta_0; \end{aligned}$$

and

$$p(t-\tau_r) = (\kappa K)^{\frac{1}{2}}Wp(t-\tau_r) + \frac{1}{\sqrt{n}}(\kappa K)^{\frac{1}{2}}K^{\frac{1}{2}}A^{-1}\mathbf{1}_n\chi(t-\tau_r);$$

$r = 1,\dots,2m$. By using (IV.1) and following the procedure in [20, Section 3.2], we can represent the closed-loop system (III.7) in new reduced order coordinates by

$$\begin{aligned} \dot{\vartheta} &= \omega; \\ M\dot{\omega} &= -D(\omega - \mathbf{1}_n\omega^d) + P^{\text{net}} - rU(\vartheta) - (\kappa K)^{\frac{1}{2}}Wp \\ &\quad - A^{-1}\mathbf{1}_n\mathbf{1}_n^\top A^{-1}(\omega - \mathbf{1}_n\omega^d t) - \sqrt{n}\,\kappa^{-\frac{1}{2}}A^{-1}\mathbf{1}_n\vartheta_0; \\ \dot{p} &= \kappa^{\frac{1}{2}}W^\top K^{\frac{1}{2}}(\omega - \mathbf{1}_n\omega^d) \\ &\quad - W^\top K^{\frac{1}{2}}A\sum_{r=1}^{2m} T_r A K^{\frac{1}{2}}Wp(t-\tau_r); \end{aligned} \tag{IV.6}$$

where we have expressed the variable $\chi$ in (IV.1) in terms of $\vartheta, \omega^d, \vartheta_0$ and $p_0$, see (IV.4).

We make the following standard assumption [20], [38].

**Assumption IV.1.** *The system* (IV.6) *possesses a synchronized motion.*

With Assumption IV.1, we define the error states

$$\tilde{\vartheta} = \vartheta - \vartheta^s; \quad \tilde{\omega} = \vartheta_0 - \vartheta_0^s + \int_0^t \tilde{\omega}(\sigma)\,d\sigma;$$
$$\tilde{p} = p - p^s; \quad x = \operatorname{col}(\tilde{\vartheta}, \tilde{\omega}, \tilde{p}).$$

Furthermore, for the $L_2$-gain performance in the controller synthesis, we assume that both the communication and electrical layers are exposed to disturbances $d_\omega : \mathbb{R}_{\geq 0} \to \mathbb{R}^n$; $d_\omega \in L_{2e}^n$, $d_p : \mathbb{R}_{\geq 0} \to \mathbb{R}^{n-1}$, $d_P \in L_{2e}^{n-1}$, respectively and, inspired by [12], define the performance output of the closed-loop system as

$$y = \begin{bmatrix} W_1^{\frac{1}{2}}\tilde{\omega} \\ W_2^{\frac{1}{2}}\tilde{p} \end{bmatrix};$$

where the weighting matrix

$$W_1 = M > 0 \tag{IV.7}$$

accounts for the system's kinetic energy and the matrix

$$\begin{aligned} W_2 &= W^{>} K^{\frac{1}{2}} W_2 K^{\frac{1}{2}} W; \\ W_2 &= I_n \quad \frac{1}{1_n^{>} A^{\ 1} 1_n} A^{\frac{1}{2}} 1_n 1_n^{>} A^{\frac{1}{2}}; \end{aligned} \tag{IV.8}$$

quantifies the deviation of the controller states (in error coordinates) from their average (scaled by $^{1}A^{\frac{1}{2}}$).

Then, the error system corresponding to (IV.6) is given by

$$\begin{aligned} \tilde{} &= \dot{}; \\ M\dot{} &= D\dot{} \quad r U(\tilde{} + {}^{s}) + r U({}^{s}) \quad (K)^{\frac{1}{2}} W p \\ &\quad \frac{1}{} A^{\ 1} 1_n 1_n^{>} A^{\ 1} \tilde{} + d_{!}; \\ p &= {}^{\frac{1}{2}} W^{>} K^{\frac{1}{2}} \dot{} \\ &\quad W^{>} K^{\frac{1}{2}} A \quad {}^{2Xm} \quad T_r A K^{\frac{1}{2}} W p(t \quad {}_r) \quad + d_p; \\ y &= \begin{bmatrix} W_1^{\frac{1}{2}} \dot{} \\ W_2^{\frac{1}{2}} p \end{bmatrix}; \quad d = \begin{bmatrix} d_{!} \\ d_p \end{bmatrix}: \end{aligned} \tag{IV.9}$$

Moreover, with Assumption IV.1, the system (IV.9) has an equilibrium point $x^{s} = \mathrm{col}(\tilde{}^{s}; \dot{}^{s}; p^{s})$ at the origin. Recall that $!^{s}$ and $p^{s}$ are uniquely given by (III.8). Hence, for any fixed ${}_0$ asymptotic stability of $x^{s}$ implies that any solution $\mathrm{col}( \ ; ! ; p)$ of the original system (III.7) with an initial condition that satisfies

$${}_0 = \frac{1}{2}1_n^{>} A^{\ 1} \quad {}^{1} K^{\ 1} p_0 \quad {}_0 \ ;$$

converges to a synchronized motion $\mathrm{col}( {}^{s}; !^{s}; p^{s})$ with initial angles satisfying

$${}_0 = \frac{1}{2}1_n^{>} A^{\ 1} \quad {}^{1} K^{\ 1} p^{s} \quad {}^{s}_0 \ :$$

This applies for any value of ${}_0$. Moreover, the dynamics in (IV.9) are independent of ${}_0$. Consequently, $x^{s}$ being asymptotically stable implies that all solutions of the original system (III.7) converge to a synchronized motion.

### B. Problem Statement

As outlined in Section I, we seek to develop a design procedure for the consensus-based secondary frequency controller (III.6) that ensures robustness with respect to heterogeneous fast-varying communication delays and simultaneously provides the option to trade off $L_2$-gain performance against the number of required communication links. The desired robustness properties are accounted for in our approach by using the LK and descriptor methods together with a $L_2$-gain dissipation inequality for time-delay systems, see Definition II.2 and [Chapters 4 and 5][26]. Compared to [26] we apply these methods to the nonlinear system (IV.9).

The number of communication links could be minimized by means of the 0-norm of the vector $Z1_m$, i.e., $kZ1_m k_0 = \#\{\text{number of } z_i | z_i \neq 0\}$ (recall from (II.2) that $Z \quad 0$ is a diagonal matrix). Yet, the difficulty in using this approach is that the resulting optimization problem is non-convex. Hence, to overcome the non-convexity, we follow [29], [31], [32] and use the $\ell_1$-norm $kZ1_m k_1 = \sum_{i=1}^{m} |z_i|$ as a convex relaxation of the 0-norm. This is motivated by the fact the $\ell_1$-norm is the convex envelope of the 0-norm and therefore its best convex relaxation [31], [32]. To further improve this relaxation, the reweighted $\ell_1$-norm $kW_Z Z1_m k_1$ can be used [32], where the diagonal entries of the diagonal matrix $W_Z$ are chosen as

$$w_{Z;i} = (z_i + \ )^{\ 1}; \quad i = 1; : : : ; m; \tag{IV.10}$$

with being a small positive number. This, however, implies that an iteration scheme is needed, since the assigned values of the weighting matrix $W_Z$ depend on the solution of the optimization problem. Alternatively, in the MG case power system engineering insights could be used to determine the weighting matrix $W_Z$, see also [31].

The above discussion leads to the following problem formulation.

**Problem IV.2.** *Consider the system* (IV.9) *with Assumption IV.1. Determine and $Z$; such that given $h_{0_r} \in \mathbb{R}_{>0}$; $h_{1_r} \in \mathbb{R}_{>0}$ with $h_{0_r} \quad {}_r(t) \quad h_{1_r}$; $r = 1; : : : ; 2m$;*

*$x^{s} = 0_{3n \ 1}$ is a uniformly asymptotically stable equilibrium point of the system* (IV.9)*,*
*the system* (IV.9) *is dissipative with respect to the supply rate $s(d; y) = \frac{1}{2}( \ ^{2}kdk_2^2 \quad kyk_2^2)$; where $d$ and $y$ are given in* (IV.9)*,*
*and the number of communication links is minimized, i.e.,* $\min_{Z \ 0} \mathrm{trace}(Z)$*:*

### C. Main Result

To present our main result, it is convenient to introduce the scaled matrix of edge weights and the corresponding scaled interconnection matrices of the communication network, i.e.,

$$Z = \ Z; \qquad T_r = W^{>} K^{\frac{1}{2}} A B_r Z B^{>} A K^{\frac{1}{2}} W: \tag{IV.11}$$

Our main result is the following solution to Problem IV.2.

**Theorem IV.3.** *Consider the system* (IV.9) *with Assumption IV.1. Recall the weighting matrices $W_1$ and $W_2$ given in* (IV.7) *and* (IV.8)*, respectively. Fix constants $0 < h_{0_r} \quad h_{1_r}$, $r = 1; : : : ; 2m$; $K > 0$ and $" > 0$ as well as weighting parameters $> 0$; $> 0$ and a diagonal weighting matrix $W_Z > 0$. Suppose that there exist parameters $> 0$ and $> 0$ and matrices $Z \quad 0$; $P > 0$, $R_{0_r} > 0$; $R_{1_r} > 0$; $S_{0_r} > 0$; $S_{1_r} > 0$ and $S_{12_r}$, such that the following optimization problem is feasible:*

$$\min_{\gamma,\ \Lambda,\ Z} \quad \gamma + \mathrm{trace}\ W_Z Z$$

*subject to*

$$Q = \begin{bmatrix} Q_{11} & 0 & Q_{13} & 0 & 0 & 0 & \frac{1}{2}I_n & 0 \\ & Q_{22} & Q_{23} & Q_{24} & Q_{25} & 0 & 0 & \frac{1}{2}I_{n-1} \\ & & Q_{33} & 0 & Q_{35} & 0 & 0 & \frac{1}{2}I_{n-1} \\ & & & Q_{44} & Q_{45} & S_{12} & 0 & 0 \\ & & & & Q_{55} & Q_{56} & 0 & 0 \\ & & & & & Q_{66} & 0 & 0 \\ & & & & & & Q_{77} & 0 \\ & & & & & & & Q_{88} \end{bmatrix} < 0; \tag{IV.12}$$

*where*

$$\begin{aligned}
&S_0 = \mathit{blockdiag}(S_{0_r}); \quad R_0 = \mathit{blockdiag}(R_{0_r}); \\
&S_1 = \mathit{blockdiag}(S_{1_r}); \quad R_1 = \mathit{blockdiag}(R_{1_r}); \\
&S_{12} = \mathit{blockdiag}(S_{12_r}); \quad Q_{11} = \Lambda D + \frac{1}{2}W_1; \\
&Q_{13} = \frac{1}{2}\Gamma - K^{\frac{1}{2}}W; \quad Q_{22} = \sum_{r=1}^{2m} S_{0_r} - \sum_{r=1}^{2m} R_{0_r} + \frac{1}{2}W_2; \\
&Q_{23} = P - \frac{1}{2}I_{n-1}; \quad Q_{24} = \begin{bmatrix} R_{0_1} & \cdots & R_{0_{2m}} \end{bmatrix}; \\
&Q_{25} = \begin{bmatrix} -\frac{1}{2}T_1 & \cdots & -\frac{1}{2}T_{2m} \end{bmatrix}; \\
&Q_{33} = -\Gamma I_{n-1} + \sum_{r=1}^{2m} h_{0_r}^2 R_{0_r} + \sum_{r=1}^{2m} (h_{1_r} - h_{0_r})^2 R_{1_r}; \\
&Q_{35} = \begin{bmatrix} -\frac{1}{2}T_1 & \cdots & -\frac{1}{2}T_{2m} \end{bmatrix}; \\
&Q_{44} = -S_0 + S_1 - R_0 - R_1; \quad Q_{45} = Q_{56} = -R_1 - S_{12}; \\
&Q_{55} = -2R_1 + S_{12} + S_{12}^\top; \quad Q_{66} = -R_1 - S_1; \\
&Q_{77} = -\frac{1}{2}\Lambda I_n; \quad Q_{88} = -\frac{1}{2}\Lambda I_{n-1};
\end{aligned}$$

*with* $T_r$ *being defined in* (IV.11) *and*

$$\begin{bmatrix} R_1 & S_{12} \\ & R_1 \end{bmatrix} \geq 0. \tag{IV.13}$$

*Choose the controller parameters as*

$$\Gamma = \Lambda^2; \quad T_r = -B_r Z B^\top. \tag{IV.14}$$

*Then, for all* $\tau_r(t) \in [h_{0_r}; h_{1_r}]$, *the origin is a locally uniformly asymptotically stable equilibrium point of the system* (IV.9) *and the system has a small-signal* $\mathcal{L}_2$*-gain less than or equal to* $\gamma = \sqrt{\rho}$ *with respect to the supply rate* $s(d,y) = \frac{1}{2}\gamma^2\|d\|_2^2 - \|y\|_2^2$; *where* $d$ *and* $y$ *are given in* (IV.9).

*Proof.* The proof is established by combining ideas of the related stability *analysis* conducted in [20] with the *control design* approach using the descriptor method, which has been applied previously to linear time-delay systems, see, e.g., [26]. By noting that the delays appear only in $p$; consider the LKF

$$\begin{aligned}
V(x; \dot{x}; t) &= V_1 + \sum_{r=1}^{2m} V_{2_r}; \\
V_1 &= \frac{1}{2}\dot{\xi}^\top(t)M\dot{\xi}(t) + U(\tilde{\xi}(t) + \xi^s) - \nabla U(\xi^s)^\top\tilde{\xi}(t) \\
&\quad + p^\top(t)Pp(t) + \frac{\Lambda}{2}(1_n^\top A^{-1}\tilde{\xi}(t))^2 \\
&\quad + \dot{\xi}^\top(t)M1_n1_n^\top A^{-1}\tilde{\xi}(t) \\
&\quad + \dot{\xi}^\top(t)AM^{-1}\left(\nabla U(\tilde{\xi}(t) + \xi^s) - \nabla U(\xi^s)\right); \\
V_{2_r} &= \int_{t-h_{0_r}}^{t} p^\top(s)S_{0_r}p(s)ds + \int_{t-h_{1_r}}^{t-h_{0_r}} p^\top(s)S_{1_r}p(s)ds \\
&\quad + h_{0_r}\int_{-h_{0_r}}^{0}\int_{t+\theta}^{t} p^\top(s)R_{0_r}p(s)ds\,d\theta \\
&\quad + (h_{1_r} - h_{0_r})\int_{-h_{1_r}}^{-h_{0_r}}\int_{t+\theta}^{t} p^\top(s)R_{1_r}p(s)ds\,d\theta;
\end{aligned} \tag{IV.15}$$

where $\rho > 0$; $P > 0$; $S_{0_r} > 0$; $S_{1_r} > 0$; $R_{0_r} > 0$; and $R_{1_r} > 0$.

The function $V_1$ consists of the traditional kinetic and potential energy terms $\frac{1}{2}\dot{\xi}^\top M\dot{\xi}$ and $U(\tilde{\xi}(t) + \xi^s)$, respectively, together with a Bregman term to center the Lyapunov function [11] as well as a quadratic term in the reduced controller states $p$. Furthermore, a Chetaev-type cross term between $\dot{\xi}$ and $\tilde{\xi}$ is added, which - as shown in the sequel - is essential to ensure that $\dot{V}$ is strictly negative definite. The functions $V_{2_r}$ are designed to account for the presence of interval fast-varying communication delays [26].

At first, we show that $V$ in (IV.15) is strict locally positive definite. The gradient of $V_1$ is given by

$$\nabla V_1 = \begin{bmatrix} v_1 \\ v_2 \\ 2Pp \end{bmatrix}; \tag{IV.16}$$

with

$$\begin{aligned}
v_1 &= \nabla U(\tilde{\xi} + \xi^s) - \nabla U(\xi^s) + \Lambda\nabla^2 U(\tilde{\xi} + \xi^s)^\top MA\dot{\xi} \\
&\quad + \Lambda(A^{-1}1_n1_n^\top A^{-1})\tilde{\xi} + \Lambda A^{-1}1_n1_n^\top M\dot{\xi}; \\
v_2 &= M\dot{\xi} + AM\left(\nabla U(\tilde{\xi} + \xi^s) - \nabla U(\xi^s)\right) + M1_n1_n^\top A^{-1}\tilde{\xi}.
\end{aligned}$$

Clearly, at the equilibrium point $x^s = 0_{3n-1}$, $\nabla V_1 = 0_{3n-1}$. Moreover the Hessian of $V_1$ evaluated at $x^s$ is given by

$$\nabla^2 V_1|_{x^s} = \begin{bmatrix} v_{11} & v_{12} & 0 \\ & M & 0 \\ & & 2P \end{bmatrix}; \tag{IV.17}$$

where

$$\begin{aligned}
v_{11} &= \nabla^2 U(\xi^s) + \Lambda A^{-1}1_n1_n^\top A^{-1}; \\
v_{12} &= AM\nabla^2 U(\xi^s) + M1_n1_n^\top A^{-1}.
\end{aligned} \tag{IV.18}$$

It is well-known that with Assumption IV.1, $\nabla^2 U(\xi^s)$ is a Laplacian matrix with $\ker(\nabla^2 U(\xi^s)) = \mathrm{span}(1_n)$ [20], [38]. Furthermore, $A^{-1}1_n1_n^\top A^{-1}$ is a positive semidefinite matrix and $\ker(A^{-1}1_n1_n^\top A^{-1}) \cap \ker(\nabla^2 U(\xi^s)) = 0_n$. In addition,

$M$ is a diagonal matrix with positive diagonal entries and $P > 0$. Thus, all block-diagonal entries of $r^2 V|_{x^s}$ are positive definite. This implies that there is a sufficiently small $\quad > 0$ such that for all $\quad 2]0;\ ]$ we have that $r^2 V|_{x^s} > 0$. Furthermore, $S_{0_r}$; $S_{1r}$; $R_{0_r}$; and $R_{1_r}$ in $V_{2_r}$ are positive definite matrices. Therefore, $x^s$ is a strict minimum of $V$.

Recall that we seek to design controller gains, such that the $L_2$-gain of the system (IV.9) is minimized while also ensuring delay robustness. By using [26, Lemma 4.3], this translates to the following constraint optimization problem

$$\begin{aligned} &\min \\ &\text{subject to} \\ &\dot{V}(x;\dot{x};t) \quad \frac{1}{2} \quad {}^2 k d(t) k_2^2 \quad k y(t) k_2^2 \qquad \% \ k x(t) k_2^2 + k d(t) k_2^2 \ ; \end{aligned}$$

where $\dot{V}$ denotes the time-derivative of the LKF $V$ in (IV.15) and % is some positive constant. Differentiating $V$ yields

$$\begin{aligned} \dot{V} &= \dot{V}_1 + \sum_{r=1}^{2m} \dot{V}_{2_r}; \\ \dot{V}_1 &= \quad \dot{+}^{\top} D \dot{+} \quad \tfrac{1}{2} \dot{+}^{\top} K^{\frac{1}{2}} W \beta + \dot{+}^{\top} d_! + \beta^{\top} P \beta + \beta^{\top} P \beta \\ &\quad + \dot{+}^{\top} A M \ r^2 U(\tilde{} + \ ^s) \dot{+} \\ &\quad \dot{+}^{\top} D A \quad r U(\tilde{} + \ ^s) \quad r U(\ ^s) \\ &\quad + \ d_!^{\top} A \quad r U(\tilde{} + \ ^s) \quad r U(\ ^s) \\ &\quad \beta^{\top} W^{\top} (\ K)^{\frac{1}{2}} A \quad r U(\tilde{} + \ ^s) \quad r U(\ ^s) \\ &\quad r U(\tilde{} + \ ) \quad r U(\ ^s)^{\top} A \quad r U(\tilde{} + \ ^s) \quad r U(\ ^s) \\ &\quad + \ \dot{+}^{\top} M 1_n 1_n^{\top} A^{\ 1} \dot{+} \quad \dot{+}^{\top} D 1_n 1_n^{\top} A^{\ 1} \tilde{} \\ &\quad \beta^{\top} W^{\top} (\ K)^{\frac{1}{2}} 1_n 1_n^{\top} A^{\ 1} \tilde{} + \ d_!^{\top} 1_n 1_n^{\top} A^{\ 1} \tilde{} \\ &\quad - \tilde{}^{\top} A^{\ 1} 1_n 1_n^{\top} A^{\ 1} 1_n 1_n^{\top} A^{\ 1} \tilde{}; \\ \dot{V}_{2_r} &= \beta^{\top}(t) S_{0_r} \beta(t) \quad \beta^{\top}(t \quad h_{0_r}) (S_{0_r} \quad S_{1_r}) \beta(t \quad h_{0_r}) \\ &\quad \beta^{\top}(t \quad h_{1_r}) S_{1_r} \beta(t \quad h_{1_r}) \\ &\quad + \beta^{\top}(t) \ h_{0_r}^2 R_{0_r} + (h_{1_r} \quad h_{0_r})^2 R_{1_r} \ \beta(t) \\ &\quad \int_{t \quad h_{0_r}}^{t} \beta^{\top}(s) R_{0_r} \beta(s) ds \\ &\quad (h_{1_r} \quad h_{0_r}) \int_{t \quad h_{1_r}}^{t \quad h_{0_r}} \beta^{\top}(s) R_{1_r} \beta(s) ds: \end{aligned} \tag{IV.19}$$

Since under the conditions of the theorem, the second LMI in (IV.12) is feasible, applying Jensen's inequality together with Lemma 3.3 in [26], see also [45], gives

$$\begin{aligned} &h_{0_r} \int_{t \quad h_{0_r}}^{t} \beta^{\top}(s) R_{0_r} \beta(s) ds \\ &\quad \beta(t) \quad \beta(t \quad h_{0_r})^{\top} R_{0_r} \ \beta(t) \quad \beta(t \quad h_{0_r}) \end{aligned}$$

and, likewise,

$$\begin{aligned} &(h_{1_r} \quad h_{0_r}) \int_{t \quad h_{1_r}}^{t \quad h_{0_r}} \beta^{\top}(s) R_{1_r} \beta(s) ds \\ &= \ (h_{1_r} \quad h_{0_r}) \int_{t \quad h_{1_r}}^{t \quad r(t)} \beta^{\top}(s) R_{1_r} \beta(s) ds \\ &\quad + (h_{1_r} \quad h_{0_r}) \int_{t \quad r(t)}^{t \quad h_{0_r}} \beta^{\top}(s) R_{1_r} \beta(s) ds \quad \begin{matrix} \top \\ r \end{matrix} \begin{matrix} R_{1_r} & S_{12_r} \\ & R_{1_r} \end{matrix} \ _r; \end{aligned}$$

where

$$_r = \operatorname{col}\{\beta(t \quad h_{0_r}) \quad \beta(t \quad \ _r(t)); \beta(t \quad \ _r(t)) \quad \beta(t \quad h_{1_r})\}.$$

Next, we apply the descriptor method, see [26, Chapter 3]. Let $P_2$ and $P_3$ be matrix variables and add the expression

$$\begin{aligned} 0 = 2 \ &\beta^{\top} P_2^{\top} + \beta^{\top} P_3^{\top} \\ &\left[ \tfrac{1}{2} W^{\top} K^{\frac{1}{2}} \dot{+} \quad W^{\top} K^{\frac{1}{2}} A \quad \sum_{r=1}^{2m} T_r A K^{\frac{1}{2}} W \beta(t \quad \ _r(t)) + d_p \quad \beta \right] \end{aligned}$$

to (IV.19). Furthermore, by defining

$$\begin{aligned} &= \operatorname{col}\{ \quad r U(\tilde{} + \ ^s) \quad r U(\ ^s) \ ; \ 1_n 1_n^{\top} A^{\ 1} \tilde{} \ ; \dot{+}; \\ &\quad \beta; \beta; \ _1; \ _2; \ _3; d_! ; d_p \ ; \\ &_1 = \operatorname{col}\{\beta(t \quad h_{0_1}); \ldots; \beta(t \quad h_{0_{2m}})\}; \\ &_2 = \operatorname{col}\{\beta(t \quad \ _1(t)); \ldots; \beta(t \quad \ _{2m}(t))\}; \\ &_3 = \operatorname{col}\{\beta(t \quad h_{1_1}); \ldots; \beta(t \quad h_{1_{2m}})\}; \end{aligned}$$

selecting $P_2 = \frac{1}{2} I_{n \ 1}$ and $P_3 = \ P_2 = \frac{1}{2} I_{n \ 1}$ with $" > 0$, recalling $T_r$ in (IV.11) and defining $\quad = \ ^{\frac{1}{2}}$ and $\quad = \ ^2$; we then obtain

$$\dot{V} \quad \frac{1}{2} \quad {}^2 k d k_2^2 \quad k y k_2^2 \qquad ^{\top} \begin{matrix} 0 & 0 \\ 0 & Q \end{matrix} + \qquad ; \tag{IV.20}$$

where $Q$ is given in (IV.12), and

$$= \begin{bmatrix} A & 0 & \frac{1}{2} A D & E_{14} & 0 & 0 & 0 & 0 & \frac{1}{2} A & 0 \\ & -A^{\ 1} & \frac{1}{2} D & E_{24} & 0 & 0 & 0 & 0 & \frac{1}{2} I_n & 0 \\ & & \frac{1}{2} E_{33} & 0 & 0 & 0 & 0 & 0 & 0 & 0 \\ & & & 0 & 0 & 0 & 0 & 0 & 0 & 0 \\ & & & & 0 & 0 & 0 & 0 & 0 & 0 \\ & & & & & 0 & 0 & 0 & 0 & 0 \\ & & & & & & 0 & 0 & 0 & 0 \\ & & & & & & & 0 & 0 & 0 \\ & & & & & & & & 0 & 0 \\ & & & & & & & & & 0 \end{bmatrix},$$

with

$$\begin{aligned} E_{14} = \quad &\frac{1}{2} A (\ K)^{\frac{1}{2}} W; \qquad E_{24} = \quad \frac{1}{2} (\ K)^{\frac{1}{2}} W; \\ E_{33} = &A M \ r^2 U(\tilde{} + \ ^s) + \ r^2 U(\tilde{} + \ ^s) M A \\ &+ M 1_n 1_n^{\top} A^{\ 1} + A^{\ 1} 1_n 1_n^{\top} M: \end{aligned}$$

Under the standing assumptions, $Q < 0$. Furthermore, the upper 2 2 block of is negative definite. Thus, by invoking [20, Lemma 11], we conclude that the matrix sum in (IV.20) is negative definite for some small > 0. Consequently,

$$\dot{V}(x;\dot{x};t) \quad \frac{1}{2} \quad {}^2kd(t)k^2 \quad ky(t)k^2 \qquad \% \; kx(t)k_2^2 + kd(t)k_2^2 \;;$$

for some 2 $\mathbb{R}_{>0}$ and % 2 $\mathbb{R}_{>0}$. By invoking [26, Lemma 4.3] we conclude that the origin of the system (IV.9) is locally uniformly asymptotically stable and that the system has a small-signal $L_2$-gain less than or equal to = $\bar{p}$—.

To conclude the proof, we note that the matrix $Q$ in (IV.12) is a LMI in the controller variables and $T_r$ as well as in the auxiliary variables , $R_0$; $R_1$; $S_{12}$; $S_0$ and $S_1$ with additional (fixed) tuning parameter ". Therefore, sparsity of the communication network can be included in the control design by augmenting the cost function in the optimization problem (IV.12) with the term trace $Z$ . This yields the constraint convex optimization problem (IV.12), where we have included additional weighting factors to trade off $L_2$-gain performance ( ) against frequency error convergence[1] ( ) and communication efforts ($W_Z$). □□□

**Remark IV.4.** The LKF candidate $V$ in (IV.15) differs from the one employed in our previous work [27] due to the consideration of interval heterogeneous fast-varying delays $_r$ and the inclusion of the matrix variable $P$ in the quadratic term in $\bar{p}$. As a consequence, the matrix $Q$ in (IV.12) also depends (linearly) on $P$. This additional degree of freedom together with the consideration of interval delays yields, in general, less conservative conditions as those derived in [27], see the numerical examples in Section V.

**Remark IV.5.** With regard to the feasibility of the optimization problem (IV.12) we see from the definition of the matrix $Q$ in (IV.12) that for any given $h_{0_r}$, $h_{1_r}$; $r = 1;:::;2m;$ choosing " 0, 1 and $kZk$ 1, ensures that there always exists 1 such that $Q < 0$. Hence, the optimization problem can always be parametrized, such that a feasible solution exists. However, we can also see from (IV.12) that with increasing value of $h_{1_r}$; the achievable $L_2$-gain performance is likely to deteriorate, which is to be expected (as in the considered system (IV.9) delays deteriorate the performance).

**Remark IV.6.** The optimization problem (IV.12) has been derived such that it is linear and convex in both the objective function and the constraints. Hence, it can be solved efficiently using standard numerical methods [46], [47], also for large-scale problems.

## V. Numerical Example

The performance of the proposed controller synthesis and the inherent design trade-off between the maximum guaranteed $L_2$-gain and the sparsity of the communication network are illustrated via numerical experiments on the three-phase islanded Subnetwork 1 of the CIGRE benchmark MV network [34] shown in Fig. 1.

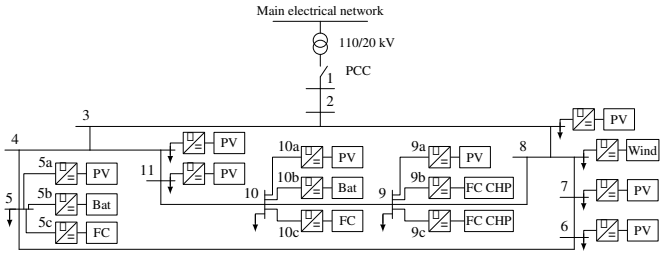


Fig. 1. 20kV MV CIGRE benchmark microgrid with 11 main buses and inverter-interfaced units of type: photovoltaic (PV), fuel cell (FC), battery, combined heat and power (CHP) FC, and wind turbine. The controlled units are located at buses 4; 5b, 5c, 6; 7; 9b, 9c, 10b, 10c and 11. PCC denotes the point of common coupling to the main grid.

The system contains 11 main buses and a total of 15 generation units. The values of the network parameters are mainly taken from [34]. Similarly to [38], the following modifications are made compared to the original system in [34]. At bus 9b, an inverter-interfaced combined heat and power (CHP) fuel cell (FC) is used instead of the CHP diesel generator. Moreover, the power ratings of the controllable generation units (CHPs, batteries, FC, PVs) are scaled by a factor 4 to be able to meet the load demand of the system in islanded mode. In order to integrate the PV units at buses 4, 6, 7 and 11 in the frequency control, we assume that they are operated at 70% of their actual maximum power point and, thus, can increase or decrease their generation. We also assume that all controllable units are equipped with frequency droop control.

Non-controlled generation units are connected at buses 3 and 8. The loads in the network represent industrial and household loads. Their data is specified in [34, Table 1]. Moreover, the largest $R/X$ ratio in the reduced admittance matrix is less than 0.3. Thus, the assumption of dominantly inductive admittances is satisfied.

To carry out the secondary control design, i.e., to solve the optimization problem (IV.12) and following our analysis, we assume that the communication between different units is affected by heterogenous fast-varying delays. To this end, we divide the network into four different groups of generation units based on the geographical distances between them, see Fig. 1. Then we assume that the communication amongst units within the same group is affected by a lower time delay than that between units from different groups (since these are located further apart). Thus, we consider delays $h_{0_1}$ = 150ms $_1(t)$ $h_{1_1}$ = 200ms between the generators 4, 5b, 5c, 11, $h_{0_2}$ = 200ms $_2(t)$ $h_{1_2}$ = 250ms between 9b, 9c, 10b, 10c, $h_{0_3}$ = 100ms $_3(t)$ $h_{1_3}$ = 150ms between the generators 6 and 7. Moreover, the maximum delay between the remaining nodes in the network is $h_{0_4}$ = 450ms $_4(t)$ $h_{1_4}$ = 500ms. Furthermore, the matrix $A$ is chosen as $A$ = diag($S_i^N$) $^1$, where $S_i^N$ = [0:0168; 0:5053; 0:0278; 0:0253; 0:0253; 0:2611; 0:1785; 0:1684; 0:0118; 0:0084] are the power ratings of the inverters in per unit (pu). We set $K$ = $D$ where

[1]In our experience, with = 0 the numerical value of resulting from the optimization problem is typically very small. This is explained by the fact that only appears in a positive off-diagonal term in $Q$ in (IV.12). Yet, when tested in simulations it turns out that a minimum value of is required to drive the frequency error to zero, thus justifying the choice > 0; see also the numerical experiments in Section V.

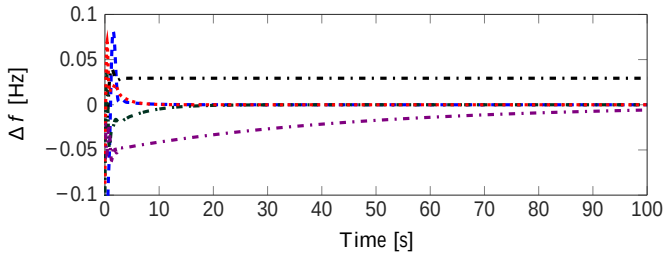


Fig. 2. Frequency convergence at bus 9b for different values of : The lines correspond to: = 1:122 10 9 '– .', = 1:1676 ' –', = 0:1844 ' ', = 0:0217 '–.', = 0:4656 '- -'

TABLE I
RESULTS FOR AND OBTAINED FROM SOLVING THE OPTIMIZATION PROBLEM (IV.12) IN 'DESIGN STEP 1' FOR DIFFERENT VALUES OF AND

| | | | | | |
|---|---|---|---|---|---|
| | 1 | 0 | 1 | 3 | 1 |
| | 0 | 1 | 1 | 1 | 3 |
| | 3.6325 | 123.598 | 3.6614 | 3.6358 | 3.7092 |
| | 1:12 10 9 | 1.1676 | 0.1844 | 0.0217 | 0.4656 |
| Number of communication links (with $W_Z = \mathbb{0}$) | 45 | 27 | 28 | 37 | 21 |

$D$ = diag(0:084; 2:526; 0:139; 0:126; 0:126; 1:305; 0:893; 0:842; 0:059; 0:042) and " = 0:3. The numerical implementation is conducted on a machine featuring an Intel Core i5-6400 with 16GB of RAM and using Matlab (R2018b), Yalmip (version 09-02-2018) [47] and the solver Mosek (version 8.1.0.51) [48].

Recall that the objective function of our proposed controller synthesis in (IV.12) is parametrized in terms of the weightings , and $W_Z$. To illustrate the effects which these different weighting parameters have on the resulting secondary frequency controller and on the closed-loop performance, we pursue a two-step case study. In the first design step, we illustrate the influence of and on the relation of the feedback gain and the estimated $L_2$-gain . This is done without enforcing any additional sparsity requirements on the communication topology (i.e., $W_Z = 0$). As a result of this first design step, we identify a nominal controller parametrization along with a nominal estimate for the $L_2$-gain. These nominal values are then used as references for the second design step, which explores the impact of reducing the number of communication links on the $L_2$-gain performance. We remark that during all design steps, robustness with respect to the specified heterogeneous fast-varying delays $_1(t); : : : ; _4(t)$ is guaranteed (as long as the optimization problem (IV.12) is feasible).

**Design step 1**. In the first step, we consider different values of and with $W_Z = 0$. The main purpose of this stage is to illustrate the necessity to include 6= 0 in the problem (IV.12). Hence, to start with, we set = 0 and solve the optimization problem (IV.12). The design problem is feasible, but yields a value for close to zero, which leads to a rather slow convergence of the frequency to its nominal value, see Fig. 2. This undesired behavior can be alleviated by setting > 0, when solving (IV.12). Furthermore, on the other extreme, setting = 0 leads to a higher value of , but a much larger upper estimate of the $L_2$-gain , which indicates a degradation of the robustness properties of the closed-loop system with respect to external perturbations. Consequently, in order to obtain a controller parametrization, which simultaneously yields fast frequency convergence and robustness > 0 and > 0 have to be chosen. Further results for and are given in Table I for different values of and . The frequency convergence for the different cases in Table I is shown for the unit at bus 9b in Fig. 2.

Since all scenarios in Table I with 6= 0 and 6= 0 have very similar $L_2$-gain performances, we simulate the closed-loop system by using the largest feedback gain, i.e., = 0:4656 and = 3:7092, for two disturbance scenarios. In the first scenario, the system is being subjected to sinusoidal disturbances $d_! = d_p = 0:2\sin(12:57t)$ [pu] in both the electrical and communication layers for $t$ 2 [1; 2], which can be interpreted as possible oscillations due to harmonics or load variations. The resulting system trajectories are shown in Fig. 3, from which it can be seen that the system returns to the original equilibrium point after the disturbances vanish. In the second disturbance scenario, a step disturbance of magnitude 0:1 [pu] starting at $t$ = 1s and lasting until $t$ = 3s is applied to the electrical layer, while simultaneously a white noise disturbance signal is applied to the communication layer. The behavior of the system trajectories is depicted in Fig. 4. Also in this case, the system trajectories remain bounded and converge to the equilibrium after the disturbances have vanished. For the present simulations, the fast-varying delays are generated by using the rate transition and variable time delay blocks in Matlab/Simulink with a sampling time $T_s$ = 2ms.

The number of required communication links is also given in Table I. It can be seen that with increasing magnitude of , the number of required links tends to decrease from 45 to around 25: Since the shape of the communication topology is a very important aspect when implementing the secondary control law (III.6), we seek to further explore its impact on the closed-loop performance in the next design step.

**Design step 2**. In light of the above observations, we select = 3:7092 and = 0:4656 as a benchmark. Then, we redesign the controller with the aim of minimizing the number of communication links while preserving robustness with respect to heterogeneous time-varying delays. Fixing and corresponds to setting = = 0 in (IV.12). The weighting matrix $W_Z$ is determined by using the reweighted $\ell_1$-norm approach [32], see also (IV.10). After solving the optimization problem (IV.12) for up to 10 iterations, in each of which the weight matrix $W_Z$ is updated, we obtain a controller with 17 communication links with the same $L_2$-gain performance as in the case of 21 communication links.

To further investigate the trade-off between the $L_2$-gain performance and the required communication efforts, we successively degrade the required $L_2$-performance by increasing the value of and then compute the necessary number of communication links by solving the optimization problem (IV.12). We find that by increasing the value of the performance index by less than 10% of , the number

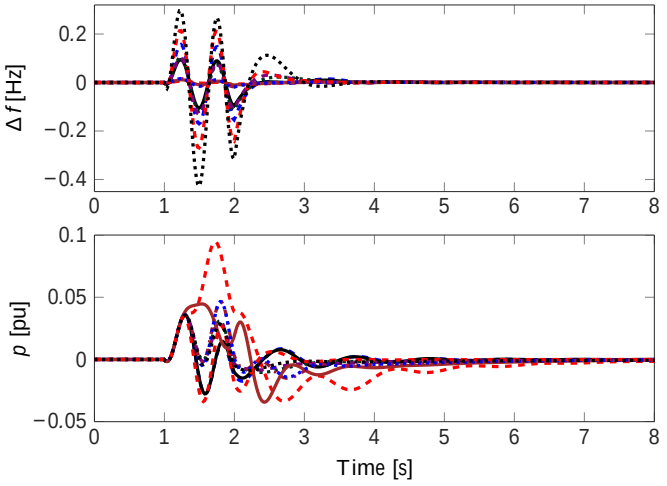


Fig. 3. Simulation results of the system (IV.9) with = 0:4656 and = 3:7092, after being subjected to sinusoidal disturbances: $d_\omega = d_p = 0{:}2\sin(12{:}57t)$ [pu] for $t \in [1; 2]$.

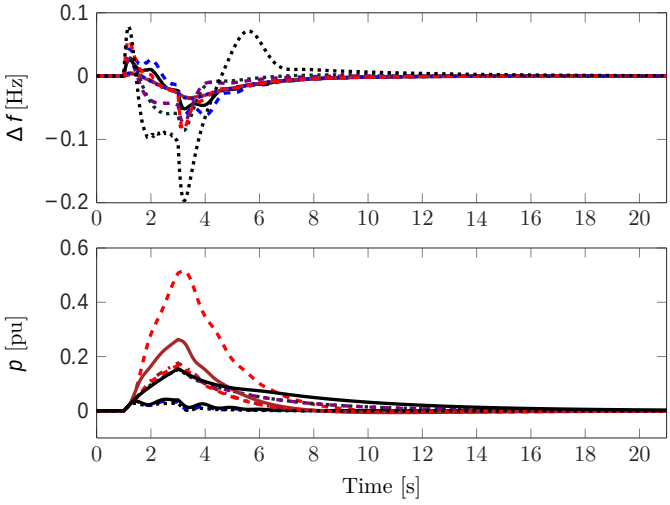


Fig. 4. Simulation results of the system (IV.9) with = 0:4656 and = 3:7092, after being subjected to disturbances: a step disturbance of magnitude 0:1 [pu] is applied to the electrical layer, while white noise is applied in the communication layer for $t \in [1; 3]$.

of communication links is further reduced from 17 to 12, see Fig. 5, which are only 3 more links than the 9 required to ensure connectivity of the communication network. Hence, we conclude that our proposed controller synthesis is well-suited to obtain practical parametrizations of the control law (III.3) that exhibit both good robustness properties and low communication requirements.

By evaluating the evolution of the non-zero entries in the Laplacian matrix $L$, illustrated in the plots in Fig. 6, we find that the controller weighting matrix $A$ seems to have a significant impact on the sparsity pattern. Namely, the unit at node 5b ($i = 2$) with the smallest entry $a_{ii}$ has the largest initial degree[2] and also preserves that degree with increasing weight on the sparsity. Compared to this, the generation unit $i = 10$,

[2]In an unweighted graph without self-loops, the degree of a node corresponds to the number of edges attached to it.

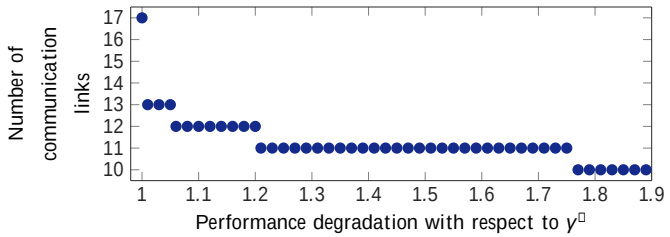


Fig. 5. Number of non-zero elements of $Z$ for different values of . The number of required communication links in the case of = 3:7092 is 17.

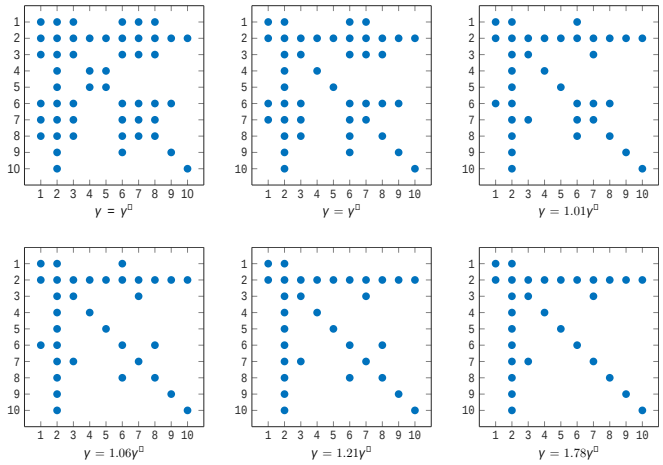


Fig. 6. Sparsity pattern of $L$ for different values of

which has the largest weight $a_{ii}$; has from the start only a degree of 1. Meanwhile, the degree of the remaining nodes is being reduced with increasing weight on the sparsity. Thereby, we observe that the communication links between generation units with larger weights $a_{ii}$ ($i = 1; 3; 5; 9; 10$) disappear first. Hence, with $A = \mathrm{diag}(S_i^N)^{-1}$ this implies that the larger generation units tend to have a higher degree of connectivity, which seems reasonable from a power engineering perspective.

The subsequent analysis is directed to further investigate how the controller parameters affect the convergence speed of the closed-loop system (III.7). To do so, we focus on the behavior of the controller state $p$. Since $A$ is fixed by economic considerations and $K = K$ where $K$ is fixed, the remaining degrees of freedom in the control design are and $L$. The effect of on the convergence speed has already been studied in design step 1 (see Table I and Fig 2). Thus, we now investigate how the sparsity of $L$ affects the convergence speed. Based on our numerical experiments, the controller states of all generation units exhibit a very similar behavior with regard to the convergence speed in dependency of the sparsity of $L$. Therefore, we use generation unit 9b ($i = 6$) as an illustrative example, since as shown in Fig. 6, that unit has access to different numbers of communication links in the different topologies obtained during the design. From simulations (with the same initial condition), we observe that the convergence speed is only slightly reduced with increasing sparsity of $L$, see Fig. 7. Based on our experience, the magnitude of has a more significant influence on the convergence speed than the shape of the communication network. This also motivated

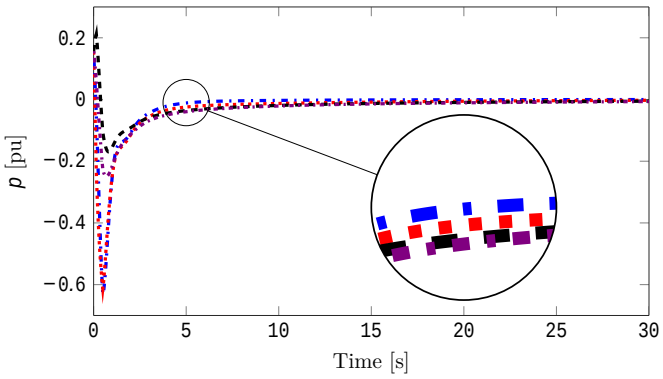


Fig. 7. The convergence of the state $p$ for generation unit 9$b$ ($i = 6$) with different numbers of communication links. The lines correspond to: No. comm. links=6 '– .', No. comm. links=4 ' ', No. comm. links=3 '- -'and No. comm. links=1 '– .'.

the inclusion of in the cost function of the optimization problem (IV.12).

Finally, we compare the conditions proposed in this paper with those derived in [27]. To this end, we use the same parameters as in [27] and consider a uniform fast-varying delay $_r(t) = (t)$ with the difference being that now we set $h_0 (t) h_1$ and $h_0 = 50$ms instead of $h_0 = 0$ as in [27]. By employing the values of and as used in [27] and solving the optimization problem (IV.12), we obtain an admissible upper bound for the communication delay of $h_{1_{\text{new}}} = 134$ ms, which corresponds to $1.34h_1$ with $h_1$ being the maximum admissible delay obtained in [27]. This shows that the proposed control synthesis with interval time-varying delays derived in the present paper permits to obtain significantly improved stability guarantees.

## VI. Conclusions

Consensus algorithms are promising control schemes for secondary control tasks in MGs. Since consensus algorithms are distributed protocols, communication efforts, disturbance attenuation and robustness with respect to time delays are significant factors for the control design and closed-loop performance. In this paper, we have jointly addressed these three challenges by proposing a design approach for a consensus-based secondary frequency controller in MGs that guarantees robustness with respect to heterogeneous fast-varying delays and simultaneously permits to trade off finite $L_2$-gain performance against the sparsity of the required communication network. More precisely, both the LKF and the descriptor methods have been applied to develop a controller synthesis in the form of a constraint convex optimization problem. The proposed synthesis guarantees uniform local asymptotic stability for any operating point satisfying the usual safety requirement of the equilibrium phase angle differences being contained in an arc of length $\frac{}{2}$.

Furthermore, the relevance of the provided weighting parameters on the resulting closed-loop behavior has been illustrated via a two-step design case study based on the CIGRE benchmark MV distribution network. The numerical results show that the proposed approach can be used to identify minimal communication topologies, while at the same time guaranteeing desired delay robustness and disturbance attenuation properties. In addition, we have shown how the weighting factors have to be chosen to facilitate a trade-off between the $L_2$-performance and the required communication efforts.

In future work, we plan to validate our design criterion experimentally and incorporate voltage and reactive power dynamics and control in the analysis. We will also investigate options to perform the control design procedure in a distributed fashion. Moreover, we will explore further applications of time-delay stability analysis and control design in MGs and bulk power systems.

## References

[1] H. Farhangi, "The path of the smart grid," *IEEE Power and Energy Magazine*, vol. 8, no. 1, pp. 18–28, 2010.
[2] G. Strbac, N. Hatziargyriou, J. P. Lopes, C. Moreira, A. Dimeas, and D. Papadaskalopoulos, "Microgrids: Enhancing the resilience of the european megagrid," *IEEE Power and Energy Magazine*, vol. 13, no. 3, pp. 35–43, 2015.
[3] J. Schiffer, D. Zonetti, R. Ortega, A. M. Stanković, T. Sezi, and J. Raisch, "A survey on modeling of microgrids—from fundamental physics to phasors and voltage sources," *Automatica*, vol. 74, pp. 135 – 150, 2016.
[4] J. A. P. Lopes, A. G. Madureira, and C. C. L. M. Moreira, "A view of microgrids," *Wiley Interdisciplinary Reviews: Energy and Environment*, vol. 2, no. 1, pp. 86–103, 2013.
[5] T. Green and M. Prodanović, "Control of inverter-based micro-grids," *Electric Power Systems Research*, vol. 77, no. 9, pp. 1204 – 1213, 2007.
[6] J. M. Guerrero, M. Chandorkar, T. Lee, and P. C. Loh, "Advanced control architectures for intelligent microgrids—part I: Decentralized and hierarchical control," *IEEE Transactions on Industrial Electronics*, vol. 60, no. 4, pp. 1254–1262, 2013.
[7] P. Kundur, *Power system stability and control*. McGraw-Hill, 1994.
[8] J. Guerrero, J. Vasquez, J. Matas, L. de Vicuna, and M. Castilla, "Hierarchical control of droop-controlled AC and DC microgrids; a general approach toward standardization," *IEEE Transactions on Industrial Electronics*, vol. 58, no. 1, pp. 158 –172, 2011.
[9] J. W. Simpson-Porco, F. Dörfler, and F. Bullo, "Synchronization and power sharing for droop-controlled inverters in islanded microgrids," *Automatica*, vol. 49, no. 9, pp. 2603 – 2611, 2013.
[10] A. Bidram, F. L. Lewis, and A. Davoudi, "Distributed control systems for small-scale power networks: Using multiagent cooperative control theory," *IEEE Control Systems Magazine*, vol. 34, no. 6, pp. 56–77, 2014.
[11] C. De Persis and N. Monshizadeh, "Bregman storage functions for microgrid control," *IEEE Transactions on Automatic Control*, vol. 63, no. 1, pp. 53–68, 2018.
[12] X. Wu, F. Dörfler, and M. R. Jovanović, "Topology identification and design of distributed integral action in power networks," in *American Control Conference (ACC)*, 2016, pp. 5921–5926.
[13] E. Tegling, M. Andreasson, J. W. Simpson-Porco, and H. Sandberg, "Improving performance of droop-controlled microgrids through distributed PI-control," in *American Control Conference (ACC)*, 2016, pp. 2321–2327.
[14] R. Olfati-Saber, J. A. Fax, and R. M. Murray, "Consensus and cooperation in networked multi-agent systems," *Proceedings of the IEEE*, vol. 95, no. 1, pp. 215–233, 2007.
[15] S. Lee, C. Lee, M. Park, and O. Kwon, "Delay effects on secondary frequency control of micro-grids based on networked multi-agent," in *16th International Conference on Control, Automation and Systems (ICCAS)*, 2016, pp. 655–659.
[16] J. Lai, H. Zhou, X. Lu, X. Yu, and W. Hu, "Droop-based distributed cooperative control for microgrids with time-varying delays," *IEEE Transactions on Smart Grid*, vol. 7, no. 4, pp. 1775–1789, 2016.
[17] E. A. A. Coelho, D. Wu, J. M. Guerrero, J. C. Vasquez, T. Dragičević, Č. Stefanović, and P. Popovski, "Small-signal analysis of the microgrid secondary control considering a communication time delay," *IEEE Transactions on Industrial Electronics*, vol. 63, no. 10, pp. 6257–6269, 2016.
[18] S. Liu, X. Wang, and P. X. Liu, "Impact of communication delays on secondary frequency control in an islanded microgrid," *IEEE Transactions on Industrial Electronics*, vol. 62, no. 4, pp. 2021–2031, 2015.